

Therapist-Exoskeleton-Patient Interaction: An Immersive Gait Therapy

Emek Barış Küçüktabak,^{1,2,4,†} Matthew R. Short,^{1,3,†} Lorenzo Vianello^{1,†},
Daniel Ludvig³, Levi Hargrove^{1,2,3}, Kevin Lynch^{2,4}, Jose Pons^{1,2,3,4,5}

¹ Shirley Ryan AbilityLab, Chicago, IL, USA

² Center for Robotics and Biosystems, Northwestern University, Evanston, IL, USA

³ Department of Biomedical Engineering, Northwestern University, Evanston, IL, USA

⁴ Department of Mechanical Engineering, Northwestern University, Evanston, IL, USA

⁵ Department of Physical Medicine and Rehabilitation,
Northwestern University, Chicago, IL, USA

† These authors contributed equally and are listed in alphabetical order.

Following a stroke, individuals often experience mobility and balance impairments due to weakness and loss of independent joint control in the lower limbs. Gait recovery is a primary goal of physical rehabilitation for these individuals, traditionally achieved through high-intensity training led by a physical therapist. However, the conventional approach used by physical therapists, applying manual assistance or resistance during training, can be physically demanding and limits their ability to physically interact with the patient at multiple joints simultaneously. Robotic exoskeletons have emerged as a promising solution, enabling multi-joint support, reducing therapist strain, and offering objective performance feedback. However, typical exoskeleton control strategies limit the physical therapist’s involvement and adaptability to the patient’s needs, which may hinder clinical adoption and outcomes.

In this study, we introduce a novel gait rehabilitation paradigm based on phys-

ical Human-Robot-Human Interaction (pHRHI), in which a therapist and an individual post-stroke are each equipped with a lower-limb exoskeleton virtually connected at the hips and knees via spring-damper elements. This connection enables bidirectional physical interaction, allowing the therapist to guide the patient’s movement while receiving real-time haptic feedback. We evaluated this approach with eight chronic post-stroke patients using within-subject design, comparing the pHRHI-based training to conventional therapist-guided mobilization during treadmill walking. Results showed that the pHRHI condition led to greater joint range of motion, increased step length/height, and elevated muscle activation compared to conventional therapy, as well as high levels of self-reported motivation and enjoyment. These findings suggest that pHRHI can effectively integrate robotic precision with therapist intuition, offering a promising framework for enhancing gait rehabilitation outcomes in post-stroke populations.

Introduction

Following a stroke, individuals often experience mobility and balance impairments due to loss of independent joint control and strength deficits in the lower extremities (1, 2). During physical rehabilitation, gait recovery is a major focus for these individuals, given the importance of ambulation in activities of daily living at home and in the community (3). Current interventions primarily focus on high-intensity gait training administered by physical therapists (4). In these sessions, therapists provide hands-on support and corrections to the limbs of the patient during overground or treadmill walking.

However, this approach requires substantial physical effort from the therapist, which can lead to work-related injuries over time (5). Additionally, because therapists must use their

hands to guide and correct the patient's movements, they are limited in their ability to provide full-body cues and assessments, potentially reducing the sense of embodiment and engagement during gait therapy. Moreover, one therapist can only physically interact with a patient at a few contact points simultaneously; as a result, the therapist's guidance is often isolated to a single aspect of the patient's gait (e.g., limb advancement). For this reason, the combined effort of multiple therapists is required for complex functional training involving the coordination of multiple joints, particularly in the early stages of rehabilitation (6).

Emerging technologies, such as lower-limb exoskeletons, have been developed to address some of these challenges in gait training by enabling intensive multi-joint rehabilitation. These solutions can provide assistance or resistance to the patient at multiple contact points, reduce the number of therapists required during therapy, and decrease the therapist's effort by sustaining the patient's weight, while also providing objective measures of gait performance (4, 7, 8). Among the various exoskeleton control strategies for gait restoration, the most common approaches include assist-as-needed and error augmentation techniques. The assist-as-needed method offers adjustable support levels tailored to the patient's ability, guiding the patient's limbs to follow predefined joint trajectories. This approach is especially beneficial for severely impaired patients in the early stages of rehabilitation, as it can encourage (re)learning of asymptomatic walking patterns (4, 9, 10). Conversely, error augmentation deliberately introduces errors or resistance during training, making it better suited for higher-functioning patients. By increasing awareness of gait deviations, this approach encourages adaptation and self-correction (11, 12).

Defining optimal reference limb trajectories for exoskeleton controllers and appropriately adjusting assistance or resistance levels during therapy is challenging and remains an open question (4, 13). These control strategies often under-utilize the expertise of the physical therapist, limiting their influence on the behavior of the exoskeleton during training (14). Com-

monly, reference trajectories are computed offline based on the walking patterns of able-bodied individuals (10), which fail to adapt adequately to the patient's performance during training and across various ambulatory activities. As a result, exoskeleton-based therapy reduces the therapist's ability to provide nuanced corrections to the patient's movement, as they would in conventional gait therapy, potentially hindering the functional effects of such training as well as the adoption of this technology in clinical settings (15). Furthermore, because therapists typically rely on external observation, either directly through visualization of limb kinematics or indirectly through performance metrics, their ability to engage in embodied, intuitive guidance is limited, diminishing real-time adaptability and interaction. This underscores the need for a balanced approach that combines the benefits of exoskeleton-based therapy with the expertise of the physical therapist to enhance rehabilitation outcomes for stroke survivors.

Using robots to mediate physical interaction between humans, known as physical Human-Robot-Human Interaction (pHRHI), provides unique opportunities to merge human motor-cognitive skills with robotic capabilities (16). In this paradigm, two individuals interface with separate robotic devices that are programmed to virtually render a physical interaction medium. Typically, this medium is modeled with springs and dampers, virtually linking either the joint configurations or the end-effectors of the robots. As a result, each individual can feel and respond to their partner's movements through the forces generated by the virtual connection. Many studies have explored this paradigm during upper-limb (17–23) and lower-limb (24–30) interaction tasks, reporting promising results in terms of enhanced motor performance and increased engagement during the interaction. However, to the best of our knowledge, no studies have virtually connected a therapist and a patient using lower-limb exoskeletons to promote embodiment during a functional task, such as treadmill walking. Virtually connecting a physical therapist to their patient using exoskeleton systems could be a promising alternative to existing gait training paradigms. This approach has the potential to harmonize the expertise and intu-

ition of therapists with the precision and consistency of robots in real-time. By establishing a compatible interaction between the patient's and therapist's joints (e.g., virtually connecting the therapist's knee to the patient's knee), therapists can better embody the patient's impairments, enabling more informative assessments and more effective guidance during physical therapy.

Combining the capabilities of lower-limb exoskeletons with pHRHI, we introduce and evaluate a novel gait training approach: *Therapist-Exoskeleton-Patient* interaction (TEPI). In this study, we validate the proposed approach by using two lower-limb exoskeletons to mediate the physical interaction between a therapist and a post-stroke patient during treadmill walking. The controllers of the two exoskeletons render compliant spring-damper elements between the joints of the two users, allowing the therapist to guide the patient and receive haptic feedback of the patient's movement. The efficacy of the TEPI approach was evaluated in eight chronic stroke participants and compared to conventional manual therapy (CMT), where the therapist is seated and manually mobilizes the patient's joints. Each patient attended two sessions on separate days, one for each therapy type, consisting of 30 minutes of treadmill walking. Observations indicated that the *Therapist-Exoskeleton-Patient* interaction resulted in a larger range of motion, including longer steps and larger step height, as well as increased muscle activation compared to conventional manual therapy. At the same time, patients reported high levels of motivation and enjoyment during TEPI training, with similar levels of self-perceived exertion compared to CMT.

Results

Eight post-stroke patients participated in two separate visits involving *Therapist-Exoskeleton-Patient* interaction (TEPI) and conventional manual therapy (CMT). In the TEPI visit, both the therapist and the patient wore lower-limb exoskeletons, with virtual springs and dampers rendered between their hip and knee joints. The stiffness parameters of the virtual connection,

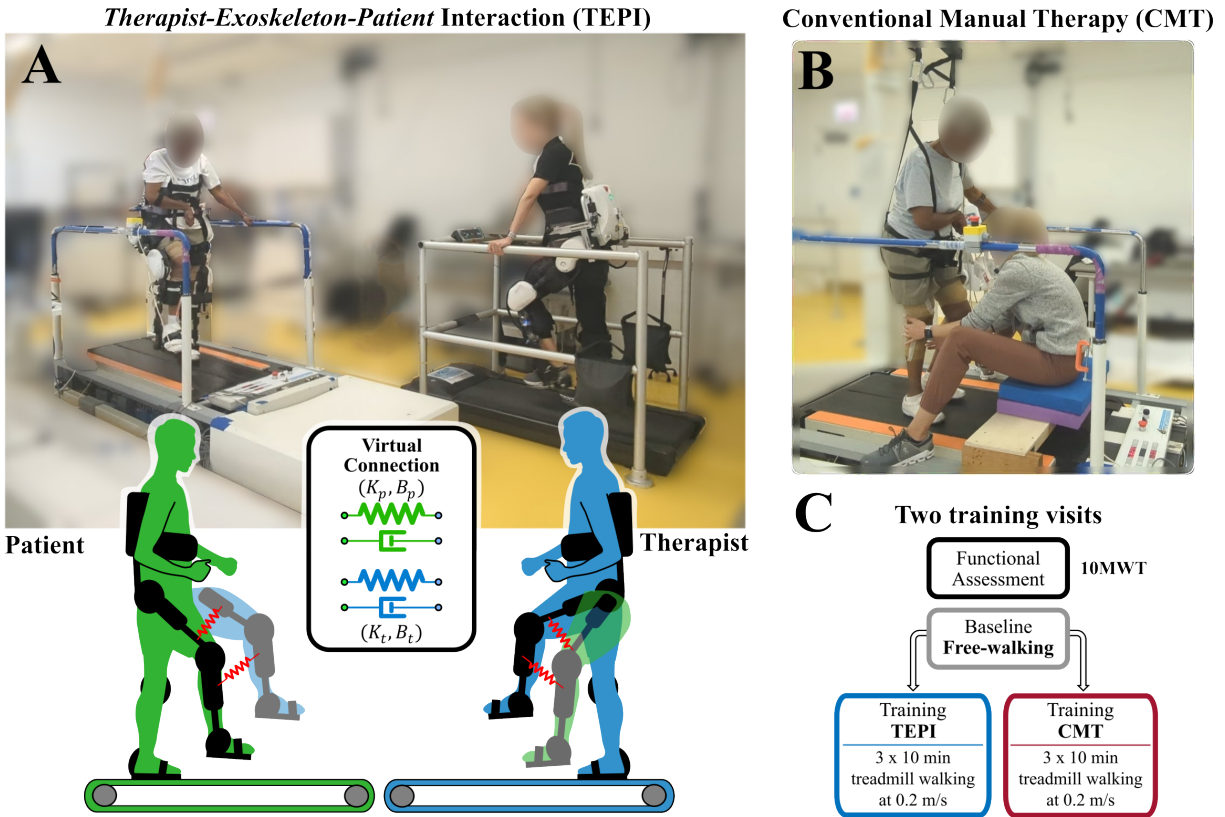


Figure 1: *Therapist-Exoskeleton-Patient* interaction (TEPI) for gait therapy: (A) a patient with chronic stroke and a physical therapist each wear lower-limb exoskeletons during a session of treadmill walking. The two exoskeletons are virtually connected via a spring-damper system that provides haptic feedback to both users. The patient and therapist face one another, altogether facilitating visual, auditory and haptic communication between the two. The TEPI approach was compared to (B) conventional manual therapy (CMT) featuring manual, hands-on assistance from the physical therapist across two training sessions conducted on separate days. (C) Each session consisted of 30 minutes of treadmill training, divided into three blocks.

reported in Supplementary Table 1, were determined on a subject-specific basis according to the physical therapist’s assessment of each patient’s needs; these parameters were adjusted as needed during the training sessions. Our framework allows us to independently change the spring-damper parameters for the patient’s exoskeleton (i.e., K_p, B_p) and the therapist’s exoskeleton (i.e., K_t, B_t), thus modifying the amount of torque feedback each partner perceives from one another. The range of virtual stiffnesses implemented was $K_p \in [49, 64]$ Nm/rad

for the patient and $K_t \in [25, 64]$ Nm/rad for the physical therapist. Damping was selected proportional to the square root of the stiffness to maintain a constant damping ratio and avoid oscillatory behaviors.

Some important outcomes of a therapy session for post-stroke patients include increasing range of motion, increasing step length and step height of the paretic limb, and maintaining high intensity (i.e., effort) during the session. We investigated how these metrics varied between TEPI and CMT sessions, where patients walked on a treadmill set to 0.2 m/s for three 10-minute blocks while receiving each type of training intervention.

Joint kinematics were used to assess the ankle's workspace area, step length, and height for both legs, as well as to measure the therapist's influence on the patient's trajectory by examining differences between their joint movements. To measure effort, we recorded bipolar electromyography (EMG) from five patients, collected from four muscles on each leg: rectus femoris (RF), biceps femoris (BF), tibialis anterior (TA), and medial gastrocnemius (MG). EMG signals from these muscles were normalized with respect to free-walking (i.e., without therapist intervention) and provided an indication of muscle activation relative to baseline walking patterns. Additionally, we used heart-rate sensors and a subjective questionnaire based on the BORG perceived rate of exertion scale (31). To assess the patients' perceived difficulty and motivation associated with the training types, we provided survey questions adapted from the Intrinsic Motivation Inventory (IMI) (32) at the end of each training session.

Therapist-patient kinematic similarity during TEPI training

The effectiveness of the TEPI approach was validated by computing the spatiotemporal similarity between the therapist's and patient's exoskeleton joint angles during training, confirming that the approach allowed the therapist to influence the patient's kinematics. An example of these joint angles during a training block, normalized in time with respect to the gait cycle, is

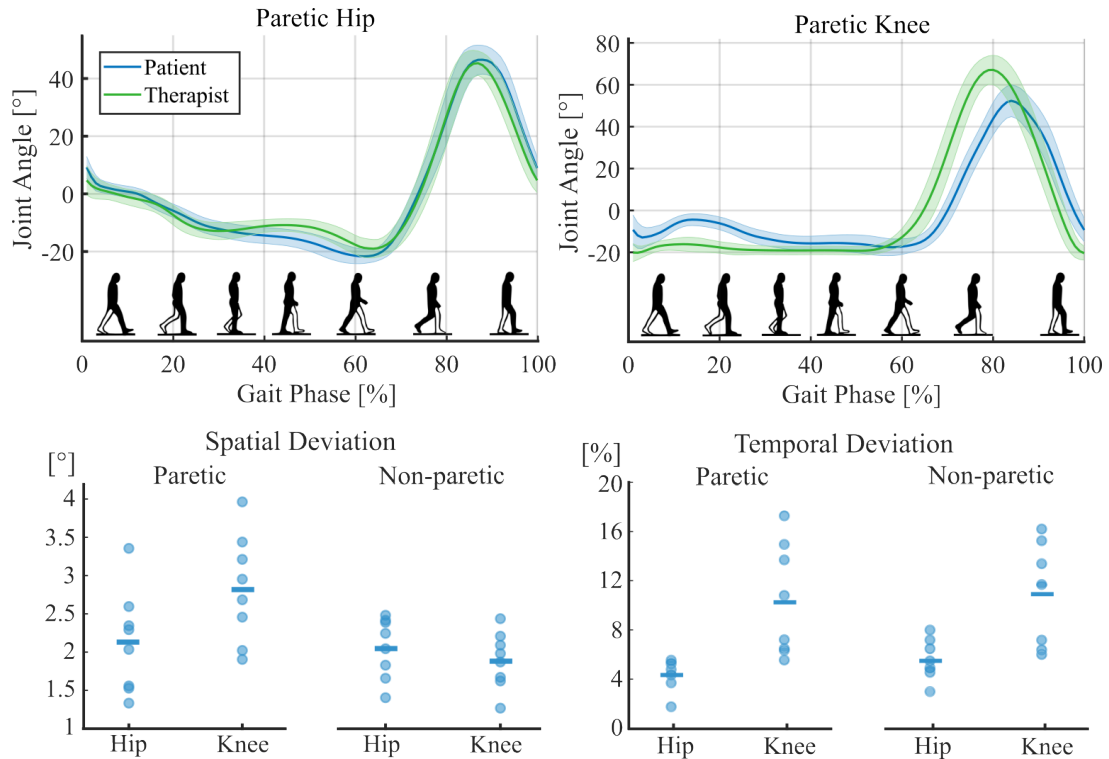


Figure 2: (Top) Representative hip and knee joint angles for the patient and therapist during a TEPI training block, time-normalized to the gait cycle. (Bottom) Spatial and temporal deviation between the joint kinematics of the therapist and patient during TEPI session. Spatial deviation (Bottom Left) was quantified as the root-mean-square-error between the joint configurations of the therapist and patient, after time-warping kinematics for each stride. Temporal deviation (Bottom Right) was quantified as time-warped lag (percentage of gait cycle) between the therapist and patient joint kinematic time-series for each stride.

presented in Figure 2 for a representative patient. During the TEPI session, the patient's trajectory closely follows the therapist's, with similar ranges of motion and temporal characteristics. For all patients and all joints, the mean spatial difference between therapist and patient was less than 4° (averaged across training blocks). On average, a larger spatial difference on the paretic side was observed compared to the non-paretic side. Regarding temporal differences, larger differences in alignment were observed at the knee joints (approximately 10% of gait cycle) compared to the hip (5% of gait cycle) for all patients.

Effects of TEPI training on spatial gait measures

To compare the effects of the TEPI training with respect to CMT, we analyzed several measures related to the spatial characteristics of patients' gait during training. To do so, we used joint angles obtained from IMU sensors placed on the thigh and shank to calculate the Cartesian coordinates of the non-paretic and paretic ankles; from these ankle trajectories, we extracted multiple parameters to compare between training conditions: workspace area, step length, and step height. Ankle trajectories of the paretic limb are shown in Figure 3, displayed for each patient and block of training for the TEPI and CMT conditions. Group data for workspace area, step length, and step height are presented for the eight patients across training blocks in Figure 4.

Workspace area (33), related to the range of motion of patients during each training intervention, was considerably larger during TEPI compared to CMT, for both the paretic (TEPI: $221.9 \pm 132.1 \text{ cm}^2$, CMT: $44.9 \pm 32.2 \text{ cm}^2$; $t_7 = 3.6$, $p < 0.01$) and non-paretic (TEPI: $236.5 \pm 133.5 \text{ cm}^2$, CMT: $71.8 \pm 36.9 \text{ cm}^2$; $t_7 = 4.0$, $p < 0.01$) legs. Across the three training blocks, this increased workspace area was relatively constant, indicating that patients were able to successfully follow the physical therapist's joint configurations for the duration of the TEPI training. We further analyzed the step length (horizontal ankle position) and step height (vertical ankle position) and obtained similar trends comparing the two training conditions. On average, step length was larger in the TEPI condition compared to CMT, for both the paretic (TEPI: $31.7 \pm 3.5 \text{ cm}$, CMT: $23.0 \pm 6.8 \text{ cm}$; $t_7 = 5.0$, $p < 0.01$) and non-paretic (TEPI: $30.5 \pm 4.6 \text{ cm}$, CMT: $20.6 \pm 6.8 \text{ cm}$; $t_7 = 7.8$, $p < 0.0001$) legs. Step height was also larger in the TEPI session, for both the paretic (TEPI: $50.5 \pm 10.0 \text{ cm}$, CMT: $34.4 \pm 10.0 \text{ cm}$; $t_7 = 3.6$, $p < 0.01$) and non-paretic (TEPI: $47.0 \pm 12.7 \text{ cm}$, CMT: $30.2 \pm 10.6 \text{ cm}$; $t_7 = 3.3$, $p < 0.05$) legs. For both training types, there was a trend of higher step length and step height for the paretic leg, compared to the non-paretic leg.

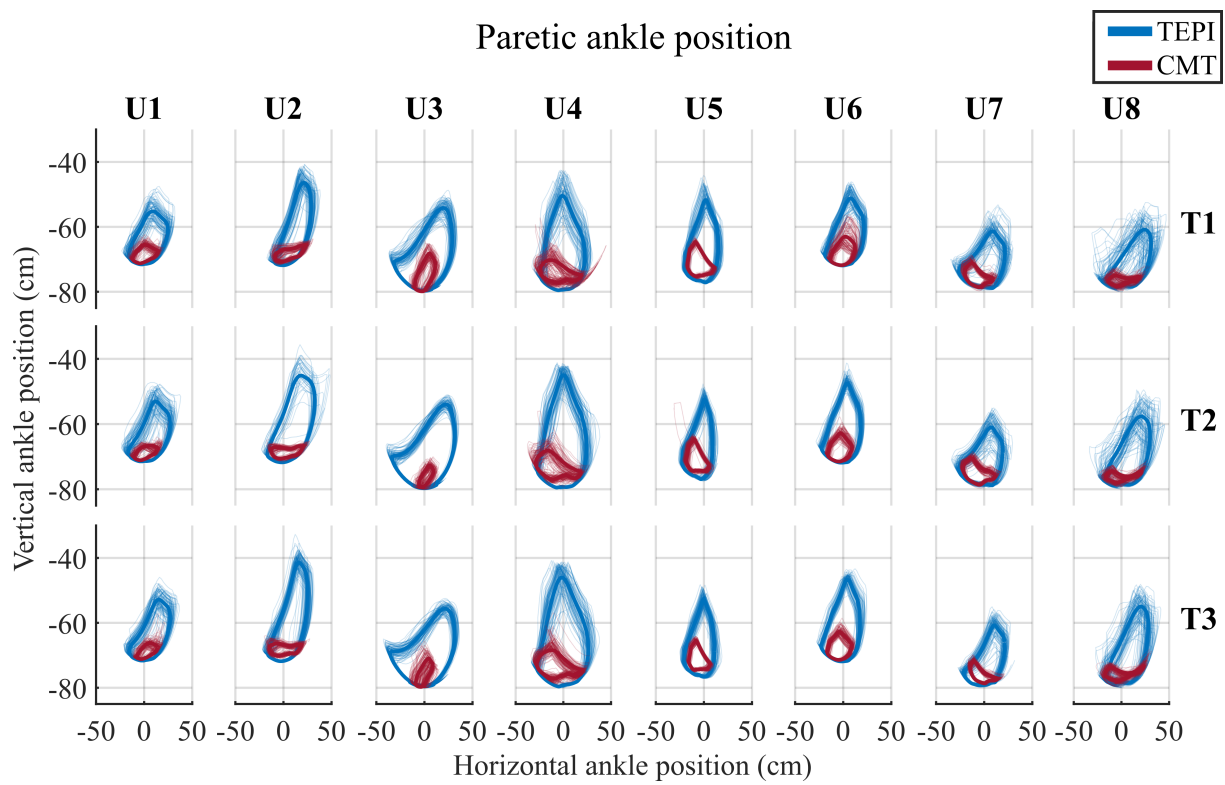


Figure 3: Paretic limb ankle trajectories for each patient (U1-U8, columns) across training blocks (T1-T3, rows), compared between the two training types: TEPI (blue) and CMT (red).

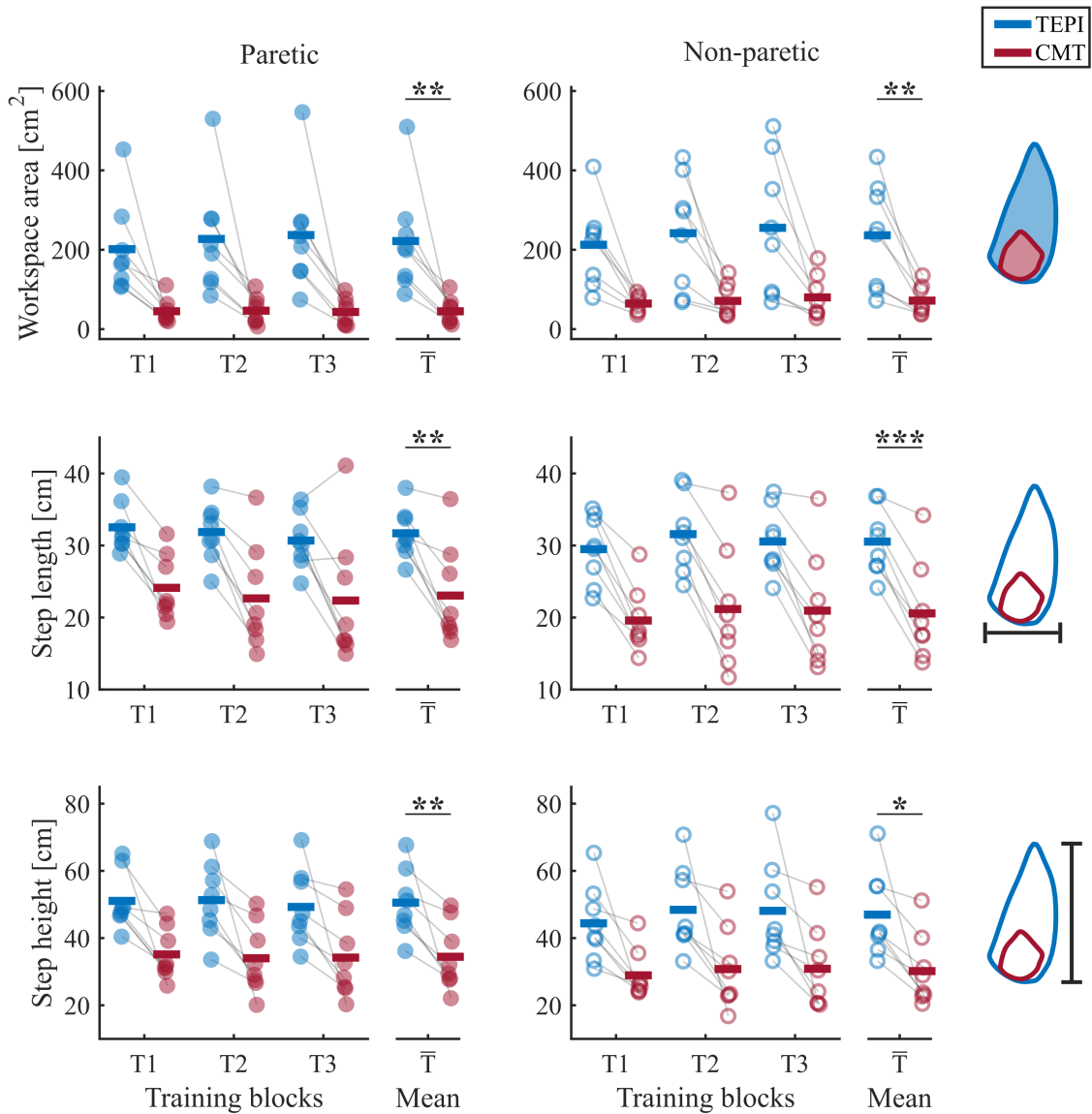


Figure 4: Spatial gait features of the paretic (Left) and non-paretic (Right) legs across training blocks (T1-T3), compared between the two training types: TEPI (blue) and CMT (red). Workspace area (first row) indicates the total area of the 2-dimensional ankle trajectory, averaged across steps within each training block. Step length (second row) indicates the horizontal distance between the landing limb and the stance limb. Step height (third row) indicates the maximum vertical distance of the swing limb with respect to the stance limb. The mean of the training blocks (\bar{T}) was used to statistically compare the two training types using paired t-tests. *, **, and *** indicate $p < 0.05$, 0.01 , and 0.001 , respectively.

Effects of TEPI training on effort

To evaluate each patient's effort during training, we analyzed mean heart rate, self-perceived measures of exertion, and muscle activation. The mean heart rate (HR) for each block within a session, as a percentage of the age-predicted maximum (34), was calculated using the formula:

$$\text{HR} = 208 - 0.7 \times \text{age}, \quad (1)$$

and is visualized in Figure 5.

During TEPI training, we observed that patient HR was higher than during CMT (TEPI: $60.4 \pm 16.3\%$, CMT: $55.7 \pm 9.6\%$; $t_7 = 1.1$, $p = 0.29$), however this difference was not statistically significant (Figure 5). Furthermore, in both conditions, HR during training was less than the target HR zone during therapy (70-85% of age-predicted maximum heart rate) for a majority of the patients. Heart rate findings were supported by the patients' perceived exertion on the 6-20 BORG scale. Patients reported higher scores on the perceived effort scale for the TEPI training (12.2 ± 4.7) compared to CMT (11.4 ± 4.2), though this trend was not statistically significant ($t_7 = 0.84$, $p = 0.43$). Notably, perceived rate of exertion tended to increase from the first to the last training block for both TEPI and CMT conditions.

In terms of muscle activation (Figure 6), we observed trends of increases in the average muscle activity, normalized with respect to free-walking, during the TEPI training compared to CMT. Across patients, this was observed as higher muscle activation for the RF (TEPI: $159.7 \pm 118.3\%$, CMT: $110.9 \pm 23.2\%$; $t_4 = 0.93$, $p = 0.4$), BF (TEPI: $225.8 \pm 99.2\%$, CMT: $107.8 \pm 45.5\%$; $t_4 = 4.0$, $p < 0.05$), TA (TEPI: $174.2 \pm 76.7\%$, CMT: $116.2 \pm 13.9\%$; $t_4 = 1.5$, $p = 0.2$) and MG (TEPI: $261.7 \pm 96.2\%$, CMT: $122.2 \pm 52.9\%$; $t_4 = 3.3$, $p < 0.05$). In general, muscle activation during TEPI training was higher than free-walking ($> 100\%$) while muscle activation during CMT training was closer to free-walking magnitudes.

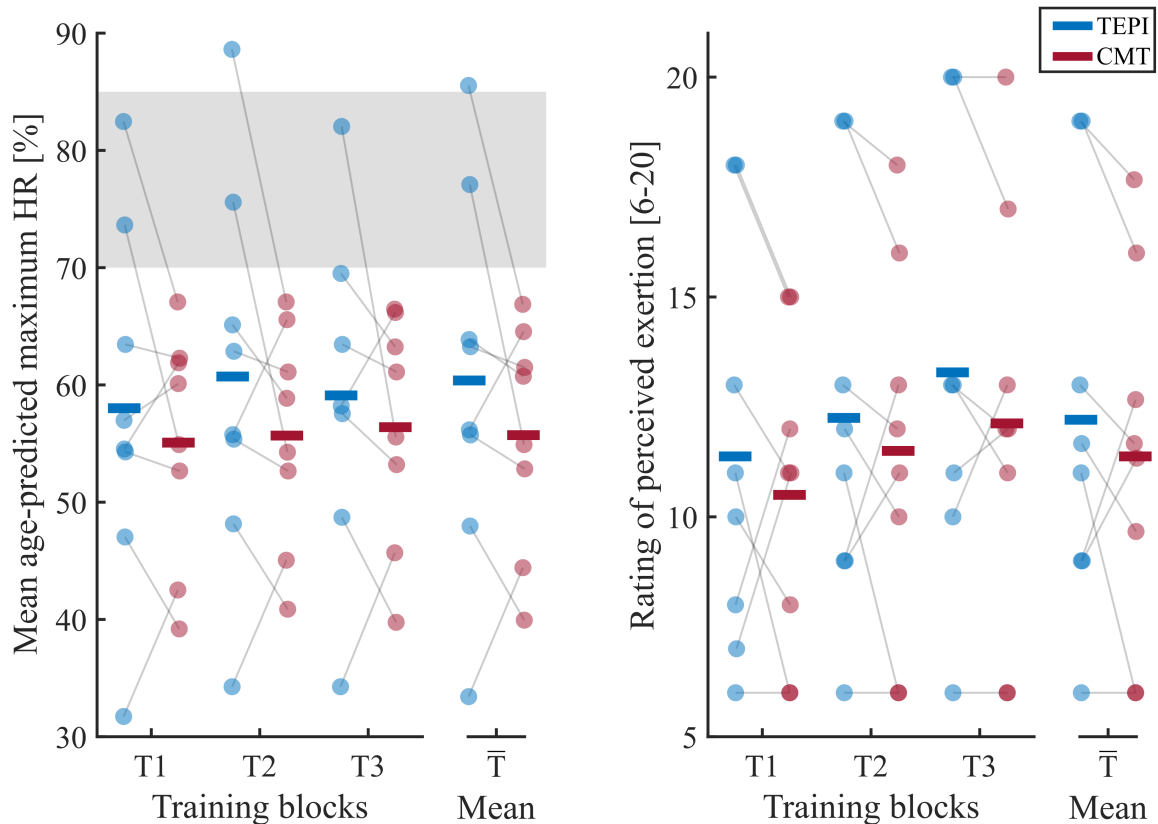


Figure 5: Patient effort across training blocks (T1-T3), compared between the two training types: TEPI (blue) and CMT (red). (Left) Mean percentage of age-predicted maximum heart rate for each session. The shaded region represents the target heart rate range during training. (Right) Rate of perceived exertion (RPE; BORG scale) reports subjective levels of effort during training, where higher values indicate greater perceived effort. The mean of the training blocks (\bar{T}) was used to statistically compare the two training types using paired t-tests.

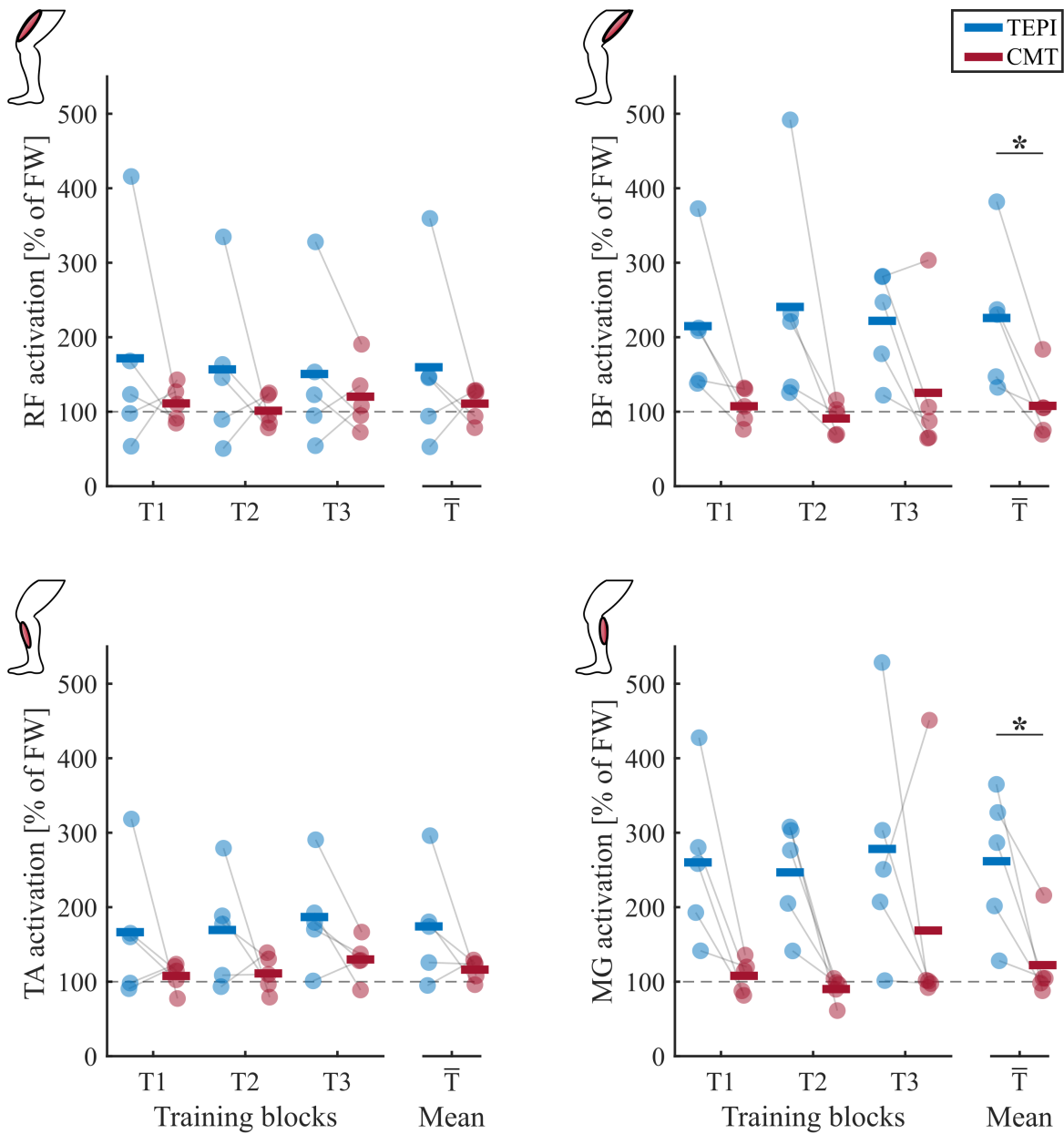


Figure 6: Average muscle activation in the paretic limb, with respect to free-walking (i.e., no training intervention), during TEPI (blue) and CMT (red) training blocks. Each point represents the mean muscle activation for a patient (U4-U8) in each training condition for each training block. 100% muscle activation indicates the mean muscle activation during free-walking. The mean of the training blocks (\bar{T}) was used to statistically compare the two training types using paired t-tests. * indicates $p < 0.05$.

Effects of training on self-reported motivation and task demand

In general, patients reported similar results for IMI survey questions related to motivation, enjoyment, and perceived difficulty of the TEPI and CMT training (Figure 7). Patients indicated that they enjoyed and had fun upon completion of both training types, with a slight, non-significant preference towards TEPI training for the **Fun** (TEPI: 5.9 ± 2.1 , CMT: 5.6 ± 1.8 ; $t_7 = 0.68$, $p = 0.52$) and **Value** (TEPI: 7.0 ± 0.0 , CMT: 6.6 ± 0.5 ; $t_7 = 2.0$, $p = 0.08$) categories. IMI scores indicated no significant differences in **Mental demand** between training types (TEPI: 2.9 ± 2.0 , CMT: 3.5 ± 2.1 ; $t_7 = -0.74$, $p = 0.48$). Other categories also showed no consistent trend across patients; feelings of **Stress** (TEPI: 1.5 ± 1.4 , CMT: 1.5 ± 1.4 ; $t_7 = 0.0$, $p = 1.0$) and **Anxiety** (TEPI: 2.1 ± 1.9 , CMT: 2.0 ± 1.9 ; $t_7 = 0.18$, $p = 0.86$) during the training remained relatively low and were comparable between the training types.

Discussion

TEPI allows the therapist to directly influence patient kinematics by applying assistance at multiple contact points

During *Therapist-Exoskeleton-Patient* interaction (TEPI), the patient's trajectory closely followed the therapist's, exhibiting similar ranges of motion and temporal characteristics. A key advantage of TEPI training is its ability to provide forces at multiple contact points, enabling a synergistic correction of both hip and knee movements during walking. Additionally, this approach provides bilateral assistance to both the stance and swing legs, simultaneously addressing key features like knee buckling, swing initiation, and weight acceptance. Achieving comparable multi-contact, bilateral assistance with manual therapy would likely require multiple therapists.

In terms of kinematics during TEPI training (Supplementary Figures 1 and 2), distinct behaviors were observed between the paretic hip and the knee joints of the patient. While the

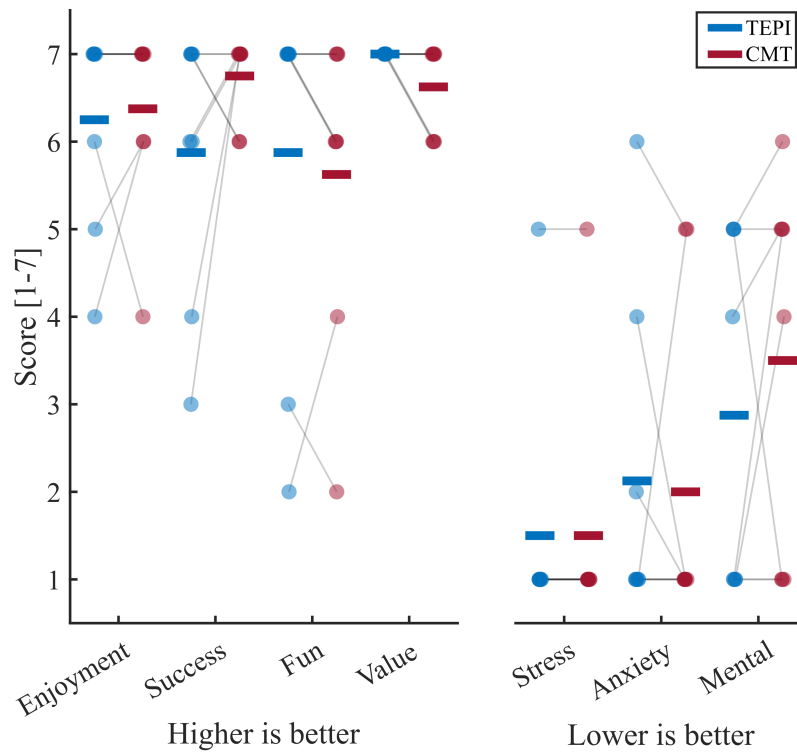


Figure 7: Patient responses to survey questions adapted from the Intrinsic Motivation Inventory (IMI) (scored from 1 to 7) for each training type: TEPI (blue), CMT (red). Higher scores indicate agreement with the feelings/descriptions associated with each question. (Left) Survey questions related to enjoyment, successful completion of the task, and value of the exercise. (Right) Survey questions related to the difficulty of the task.

patient's hip joint showed a slight temporal lead compared to the therapist's during the swing phase, the opposite relationship was observed for the knee joint. This suggests that the therapist may preferentially focus on the assistance of knee flexion to reduce compensatory strategies typically used by the patient, such as excessive hip circumduction (35, 36). This interpretation is further supported by the kinematics of the non-paretic leg, where no significant temporal lead was observed in either the hip or the knee joints, indicating a more natural and symmetric coordination in the absence of more significant impairments.

In addition, the patient demonstrated a smaller range of motion at the paretic knee compared to the therapist. This discrepancy is likely due to the increased joint stiffness of the patient's knee (37), which may have prevented them from achieving the full range of motion imposed by the therapist, even when physical interaction was present. Such limitations are consistent with the general trend in post-stroke patients, where distal joints tend to be more affected than proximal joints (38).

These findings underscore several important considerations for future research directions. First, they support the need for compliant connections in the human-robot interface to ensure patient safety, especially by avoiding overextension of impaired joints. Second, they emphasize the importance of adapting joint-level stiffness properties to the individual patient's impairments and therapeutic goals. Finally, they point toward the potential benefit of integrating assistive strategies for more distal joints, such as the ankle, to better support the full range of motor deficits experienced by patients.

Regarding temporal deviations between therapist and patient kinematics during TEPI training, larger deviations were observed at the knee joints compared to the hip. Because identical damping values were applied at both joints, the lower mass of the shank resulted in a higher damping ratio at the knee. Combined with the knee's faster angular velocity during gait, this increased damping contributed to the greater temporal lag observed at the knee.

Temporal and spatial differences in joint kinematics resulted in variations in the magnitude of the interaction torques, as shown in the Supplementary Materials (Supplementary Figures 1 and 2). Notably, greater interaction torque was observed at the non-paretic hip around 40% of the gait cycle, indicating increased therapist support to the stance leg during the swing phase of the paretic limb. Moreover, during the swing phase (60–100%), increased interaction torques were observed at both the paretic hip and knee joints. These interaction torques translated into perceived assistance or resistance for the therapist and the patient, varying by joint and gait phase, as observed in the interaction power plots in Supplementary Figures 1 and 2. Overall, these findings suggest that the therapist delivered targeted, phase-specific corrections to both legs in a more coordinated and synergistic manner than is typically achievable through manual guidance.

TEPI training allows the therapist to increase the patient’s range of motion compared to conventional rehabilitation

Compared to conventional manual therapy, *Therapist-Exoskeleton-Patient* interaction led to increased range of motion, step length, and step height in both the paretic and non-paretic legs. These findings suggest that the physical therapist was more effective in modifying patients’ movements to resemble asymptomatic walking patterns during TEPI training compared to CMT. Interestingly, in both training conditions, step length and step height tended to be larger for the paretic leg than for the non-paretic leg. This suggests that the therapist deliberately exaggerated the movement of the paretic leg during training. This approach differs from conventional exoskeleton control strategies, which typically either assist the motion as needed to complete the movement (e.g., assist-as-needed) or amplify the patient’s error (e.g., error augmentation).

While different strategies might be adopted in longer training sessions or with different pa-

tients, this observation highlights the need to reconsider exoskeleton control approaches for gait rehabilitation. The optimal control strategy for promoting neuroplasticity in neurorehabilitation remains unclear. The proposed approach could help uncover the motor mechanisms therapists instinctively target when physically interacting with patients. The holistic dataset collected during dyadic exoskeleton training, including audio-visual, kinematic, and dynamic information from both therapist and patient, is provided in the Supplementary Materials. This dataset can be leveraged by the community to identify therapist-driven control strategies and develop fully collaborative robotic controllers.

TEPI Training Promotes Active Patient Involvement

To assess patients' effort during each training session, we analyzed mean heart rate, self-perceived effort, and muscle activation. Results indicated that heart rates were relatively higher during dyadic exoskeleton training compared to conventional training. Perceived effort showed a similar trend, though results varied across patients. Notably, ratings of perceived exertion tended to increase from the first to the last training block, likely due to fatigue throughout the training session. Muscle activation was generally higher during TEPI training compared to CMT and free walking. In contrast, muscle activation during CMT was closer to that of free walking. While it is possible that this increased muscle activation can, in part, be attributed to the additional constraints imposed by the exoskeleton (i.e., movement in the sagittal plane), these results indicate that the patients were not passive during the exoskeleton training. In other words, the improved range of motion, step length, and step height noted previously were not solely due to the therapist's assistance, but also the patient's active participation in attempting to follow the therapist's guidance.

Effects of training on self-reported motivation and task demand

In general, patients reported similar results for IMI survey questions related to motivation and perceived difficulty of the TEPI and CMT sessions. Patients indicated that they enjoyed and had fun upon completion of both training types, with a slight preference towards the TEPI training in the categories of **(Fun)** and **(Value)** for most patients. In terms of cognitive load, a majority of patients reported that the TEPI training was less mentally demanding than the CMT. Other categories showed no consistent trend across patients; feelings of stress and anxiety during the training remained relatively low and were comparable between the training types. Importantly, these survey results suggest that chronic stroke patients remain motivated throughout training and do not appear deterred by the constraints imposed by exoskeleton-based assistance, viewing it as comparably acceptable to conventional manual support.

Limitations

While the comparison of our *Therapist-Exoskeleton-Patient* framework and conventional manual assistance is relevant in understanding the therapist's ability to modify their patient's kinematics during training, we acknowledge that this comparison has some limitations. For higher functioning individuals with chronic stroke, physical therapists would likely implement progressive, resistive strategies, as opposed to manual assistance, to more appropriately challenge patients during training (39). As a first step in the validation of our framework in a neurologically impaired population, we focused on higher-functioning individuals with chronic stroke and gave the physical therapist freedom to decide which specific aspects of gait to correct for each patient across visits. In addition, the proposed framework was tested during conventional, body weight-supported treadmill training, involving forward walking at speeds slower than all patient's self-selected, overground velocities. To better understand its impact and advantages, future research should explore more complex ambulatory activities. For instance, assessing this

framework during more challenging gait speeds (e.g., greater than self-selected velocity) in different overground conditions (e.g., overground walking, stairs, ramps) could provide valuable insights into how this technology may be adapted for clinical use.

While human gait primarily involves coordinated hip, knee, and ankle movements in the frontal and sagittal planes, the exoskeleton used in this study only provides sagittal plane actuation at the hip and knee joints. Expanding support to the frontal plane offers an opportunity to incorporate balance training alongside kinematics improvements. In addition, incorporating ankle assistance could enhance training of pre-swing push-off behaviors, a critical component of post-stroke gait rehabilitation (40). Using the general framework of TEPI, the integration of these additional degrees of freedom can be explored in future studies.

Another limitation of our TEPI framework compared to conventional therapy is the requirement of two exoskeleton systems, which may not always be available in clinical settings. To address this, recent studies have examined hybrid approaches where a physical therapist uses an IMU suit to teleoperate the patient's exoskeleton (41). However, this method lacks haptic feedback returned to the physical therapist, thus limiting the potential benefits of embodiment during the interaction. These two interaction types represent distinct implementations of pHRHI: unidirectional (e.g., IMU-exoskeleton) and bidirectional interaction (e.g., exoskeleton-exoskeleton). Previous work involving pHRHI during visuomotor ankle tracking has suggested similar kinematic benefits associated with unidirectional and bidirectional interaction in healthy individuals (27). However, further work is needed to validate these findings in the context of multi-joint TEPI. It would also be valuable to compare our TEPI framework with conventional exoskeleton approaches (e.g., compliant trajectory guidance (10)) to assess the added value of therapist involvement during robotic gait rehabilitation.

Although exoskeleton setup time was not formally analyzed in this study, we estimate that a therapist can set up both their own exoskeleton and the patient's exoskeleton in under 15 minutes

after initial familiarization with the systems. This setup time, while longer than conventional gait therapy, can be further reduced with prior knowledge of the patient's limb lengths. During TEPI training, future research could also examine how therapists and patients adapt their strategies while physically interacting—for example, quantifying the duration of training necessary to converge to steady-state behaviors in terms of kinematics, dynamics, and muscle activation patterns (42). It would also be interesting to examine how changes in the interaction medium (e.g., stiffness parameter combinations) influence this convergence.

Conclusion

In this study, we introduce a novel approach to gait therapy in which a therapist and a post-stroke patient each wear lower-limb exoskeletons and train together through virtual physical interaction. This approach aims to harmonize the expertise and intuition of physical therapists with the capabilities of robots, providing real-time assistance based on the physical therapist's lower-limb kinematics and their visual, auditory, and haptic assessment of the patient's behaviors. We evaluated this approach with eight chronic stroke patients and a licensed physical therapist, comparing results to conventional methods of manual assistance. Our results demonstrated that the *Therapist-Exoskeleton-Patient* interaction led to significantly greater range of motion, including larger step length and step height, and increased muscle activation compared to conventional manual assistance, as well as high levels of self-reported motivation and enjoyment. These findings suggest that incorporating physical human-robot-human interaction into therapeutic practices has the potential to improve the effectiveness of post-stroke gait rehabilitation; however, longitudinal studies are necessary to quantify the effects of such training on restoring gait function in future work.

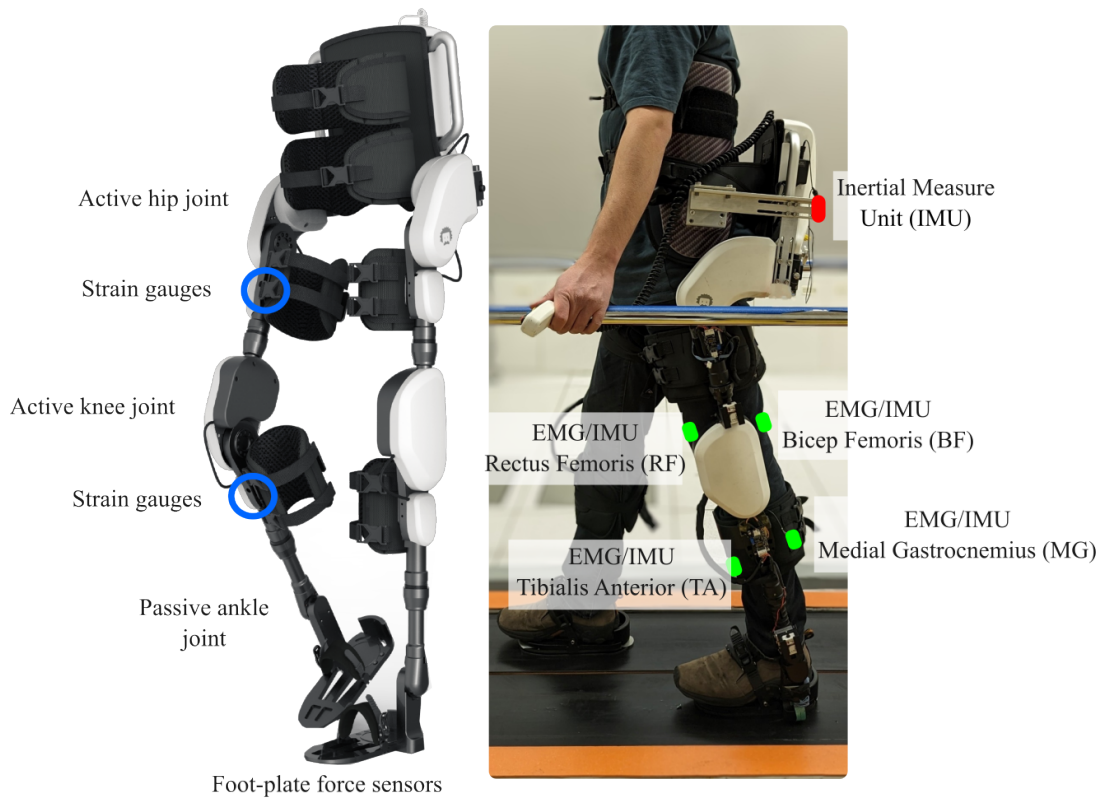


Figure 8: Fourier Intelligence ExoMotus-X2 lower-limb exoskeleton (left), and a user wearing the exoskeleton (right). On the left, we highlight key components of the exoskeleton, including four active degrees-of-freedom (DoFs) at the hips and knee joints, two passive DoFs at the ankle joints, strain gauges on the thigh and shank to measure interaction forces, and force sensors on the feet to monitor ground contact. On the right, EMG and IMU sensor placements used for both experimental conditions (i.e., TEPI, CMT) are visualized.

Materials and Methods

System Description

Two lower-limb exoskeletons (ExoMotus-X2, Fourier Intelligence), illustrated in Figure 8, were modified and implemented in our TEPI framework for gait therapy. The X2 exoskeleton, designed for overground walking, features four active degrees-of-freedom (DoFs) at the hip and knee joints, while passively supporting the ankle joints with a torsional spring.

Communication with the motors and onboard sensors was facilitated through the CAN bus

using CANOpen protocol. To minimize the communication lag, an external PC was tethered to both exoskeletons. The control systems were developed using a ROS and C++ based open-source software framework, CANOpen Robot Controller (CORC) (43), and operated at a frequency of 333 Hz on the external PC.

To render the virtual interaction medium between the two exoskeletons, we implemented torsional spring and damper elements between the hip and knee joints of the therapist and the patient. These elements determine the amount of haptic feedback perceived by the therapist and patient, and can be adjusted independently for each user. As the therapist and patient face one another during training, their opposite legs are virtually coupled. In other words, the left and right legs of the therapist are coupled with the right and left legs of the patient, respectively; this was implemented in alignment with mirror therapy approaches commonly used during gait training (44). Based on the properties of the virtual interaction elements and the instantaneous joint states of both exoskeletons (t : therapist's exoskeleton, p : patient's exoskeleton), desired interaction torques for each exoskeleton were calculated for each joint as

$$\hat{\tau}_t^* = K_t(\tilde{\theta}_p - \theta_t) + B_t(\dot{\tilde{\theta}}_p - \dot{\theta}_t), \quad (2)$$

$$\hat{\tau}_p^* = K_p(\tilde{\theta}_t - \theta_p) + B_p(\dot{\tilde{\theta}}_t - \dot{\theta}_p), \quad (3)$$

where $\hat{\tau}_i^* : i \in t, p$ are the desired interaction torques for the exoskeleton of the therapist and the patient, $(K_i, B_i) : i \in t, p$ are the stiffness and damping components, $(\theta_i, \dot{\theta}_i)$ and $(\tilde{\theta}_i, \dot{\tilde{\theta}}_i) : i \in t, p$ are the joint angles and velocities of the two opposite legs. Desired interaction torques for each joint of each user were commanded to their corresponding exoskeleton (28).

Both exoskeletons run independent instances of a whole-exoskeleton closed-loop interaction torque controller (45) to track desired interaction torques determined by the virtual interaction elements. The controller compensates for whole-body dynamics, including the full weight of the exoskeleton, and calculates the interaction torque error during the entire gait cycle. This

Table 1: Patient characteristics.

Patient	Sex	Age [years]	Height [cm]	Body-weight [kg]	Paretic Side	Time since stroke [years]	SSW Speed [m/s]
U1	F	76	160	56	Right	21	0.67
U2	M	66	163	66	Right	14	0.58
U3	M	70	178	85	Right	21	0.77
U4	M	73	175	90	Left	6	0.91
U5	F	65	165	99	Right	6	0.69
U6	M	55	170	74	Left	15	1.07
U7	F	34	170	91	Right	4	1.10
U8	M	42	180	79	Left	3	0.69

error is used as an input to a virtual admittance model that outputs desired joint accelerations. Joint accelerations are then fed into an optimization scheme to follow these commands under physical and safety constraints. Compensating for the undesired weight and inertial forces of the exoskeletons allows the therapist and patient to accurately perceive one another's forces through the rendered virtual interaction medium.

Participants and Experimental Protocol

Eight patients (60.1 ± 15.2 years) with chronic hemiparetic stroke (more than six months since onset) participated in this study. Their characteristics are detailed in Table 1. The patients gave their written consent in accordance with the Declaration of Helsinki. The study protocol (STU00212684) was approved by the Institutional Review Board of Northwestern University. The same licensed physical therapist conducted both sessions for all patients. Prior to the study experimentation, the therapist was trained to use the pHRHI platform in two familiarization sessions. In each session, the therapist performed 20-minute blocks of walking while virtually connected to a healthy pilot user. In the final phase of training, the healthy team member simulated passivity in one leg, requiring the therapists to provide corrective assistance.

Each patient attended two training visits (i.e., TEPI and CMT) separated by a minimum

of one week; the order of these visits was randomized across patients. Before and after each session of training, the patient performed three minutes of treadmill walking at 0.2 m/s without wearing an exoskeleton and without receiving any assistance from the therapist to obtain their baseline walking pattern. During these pre- and post-assessments, patient kinematics and muscle activations were recorded using EMG/IMU sensors (Trigno Avanti, Delsys).

Prior to the TEPI sessions, the exoskeleton's link lengths were individually adjusted for each patient. Following this adjustment, the session began with an initial familiarization phase during which the patient walked on the treadmill while the exoskeleton operated in haptic transparent mode (i.e., no connection to the therapist). This was followed by a second familiarization phase in which the therapist and patient were virtually connected and performed tasks together while standing (e.g., unilateral hip and knee flexion). Following the familiarization phase, three 10-minute training blocks were conducted, with approximately three-minute breaks between each session. During the training blocks, the patient and therapist faced one another, and the therapist provided physical assistance through the virtual connection of the two exoskeletons, in addition to auditory cues. Between blocks of the TEPI training session, the therapist had the flexibility to modify the amount of haptic feedback from the patient (i.e., changing K_t in Eq. 3) to provide easier control when necessary. Supplementary Table 1 displays the stiffness for each training block and each user. Due to a technical issue with the exoskeleton, one patient (U2) was only able to complete two of the three training blocks.

During the CMT sessions (Figure 1), the therapist sat in front of the treadmill and provided manual assistance to the patient, consistent with conventional body weight-supported treadmill training (46). The therapist had the freedom to interact with one or both legs, depending on her assessment of the patient's needs. Auditory cues were again provided by the therapist to facilitate the training. To provide a visual aid similar to the TEPI approach, a mirror was placed in front of the patients during CMT training.

Data Recording and Analyses

Exoskeleton kinematic data were measured at 333 Hz through encoder readings of the hip and knee joints. Additionally, wireless EMG/IMU sensors (Trigno Avanti, Delsys) were used to measure muscle activation and kinematics during both visits. Eight sensors were placed on the bellies of the following muscles in both legs: rectus femoris (RF), biceps femoris (BF), tibialis anterior (TA), and medial gastrocnemius (MG). For CMT, an additional IMU was placed on the trunk; for TEPI, an IMU sensor on the backpack of the exoskeleton was used.

EMG data were sampled at 1000 Hz. Initially, the raw EMG signals were bandpass filtered between 20 and 500 Hz using a sixth-order Butterworth filter. Subsequently, a notch filter was applied between 59 and 61 Hz to minimize noise from power-line interference. After full-wave rectification, the signals were low-pass filtered at 5 Hz. The filtered quaternion output of the Trigno sensors, sampled at 148 Hz, was used to measure joint angles in the sagittal plane. All data related to kinematics and muscle activation were windowed and time-normalized between consecutive heel-strikes, detected by ground reaction force sensors instrumented under a split-belt treadmill.

Heart rate was measured using optical heart rate sensors (Verity Sense, Polar). Additionally, after each training block, each patient reported their self-perceived rate of exertion (6-20) using the BORG scale (31).

We adapted eight questions from the IMI (32) to assess the self-reported difficulty and motivation associated with each training type. We asked patients to state their agreement or disagreement (scored from 1 to 7; 1 indicating total disagreement, 7 indicating total agreement) with the following statements:

- **Enjoyment:** I enjoyed doing this activity.
- **Success:** I was successful in accomplishing the task.

- **Fun:** I would describe this activity as fun.
- **Value:** I would be willing to do this again because it has value to me.
- **Stress:** I felt unsafe and stressed.
- **Anxiety:** I was anxious while working on this task.
- **Mental demand:** The task was mentally demanding.

Paired t-tests were used to compare the outcome measures between the two training visits: dyadic and conventional therapy. Significance was set to 0.05 for all statistical tests. Results are provided as mean \pm standard error unless otherwise specified.

Acknowledgments

We would like to thank Clement Lhoste, Hamidollah Hassanlouei, Laura Bandini, Francesco Di Tommaso, Abhishek Sankar, and Jialu Yu for their help with experimental preparations and data collection; Grace Hoo for recruiting patients; Tim Haswell for his technical support on the hardware improvements of the ExoMotus-X2 exoskeleton and Francesco Lanotte for the setup pictures

References

1. N. Arene, J. Hidler, Understanding motor impairment in the paretic lower limb after a stroke: a review of the literature, *Topics in stroke rehabilitation* **16**, 346 (2009).
2. N. Sánchez, A. M. Acosta, R. Lopez-Rosado, A. H. Stienen, J. P. Dewald, Lower extremity motor impairments in ambulatory chronic hemiparetic stroke: evidence for lower extremity weakness and abnormal muscle and joint torque coupling patterns, *Neurorehabilitation and neural repair* **31**, 814 (2017).

3. A.-S. Rudberg, *et al.*, Stroke survivors' priorities for research related to life after stroke, *Topics in stroke rehabilitation* **28**, 153 (2021).
4. J.-M. Belda-Lois, *et al.*, Rehabilitation of gait after stroke: a review towards a top-down approach, *Journal of neuroengineering and rehabilitation* **8**, 1 (2011).
5. B. McCrory, *et al.*, *Proceedings of the Human Factors and Ergonomics Society Annual Meeting* (SAGE Publications Sage CA: Los Angeles, CA, 2014), vol. 58, pp. 1072–1076.
6. K. M. Stephan, D. Pérennou, Mobility after stroke: relearning to walk, *Clinical pathways in stroke rehabilitation: evidence-based clinical practice recommendations* pp. 123–147 (2021).
7. T. Moeller, *et al.*, Use of lower limb exoskeletons as an assessment tool for human motor performance: a systematic review, *Sensors* **23**, 3032 (2023).
8. R. Gassert, V. Dietz, Rehabilitation robots for the treatment of sensorimotor deficits: a neurophysiological perspective, *Journal of neuroengineering and rehabilitation* **15**, 1 (2018).
9. B. Hobbs, P. Artemiadis, A review of robot-assisted lower-limb stroke therapy: unexplored paths and future directions in gait rehabilitation, *Frontiers in neurorobotics* **14**, 19 (2020).
10. R. Baud, A. R. Manzoori, A. Ijspeert, M. Bouri, Review of control strategies for lower-limb exoskeletons to assist gait, *Journal of NeuroEngineering and Rehabilitation* **18**, 1 (2021).
11. L. Marchal-Crespo, P. Tsangaridis, D. Obwegeser, S. Maggioni, R. Riener, Haptic error modulation outperforms visual error amplification when learning a modified gait pattern, *Frontiers in neuroscience* **13**, 61 (2019).

12. L. Marchal-Crespo, D. J. Reinkensmeyer, Review of control strategies for robotic movement training after neurologic injury, *Journal of NeuroEngineering and Rehabilitation* **6** (2009).
13. J. Zhang, *et al.*, Human-in-the-loop optimization of exoskeleton assistance during walking, *Science* **356**, 1280 (2017).
14. C. J. Hasson, J. Manczurowsky, E. C. Collins, M. Yarossi, Neurorehabilitation robotics: how much control should therapists have?, *Frontiers in Human Neuroscience* **17**, 1179418 (2023).
15. C. Celian, *et al.*, A day in the life: a qualitative study of clinical decision-making and uptake of neurorehabilitation technology, *Journal of neuroengineering and rehabilitation* **18**, 1 (2021).
16. E. B. Küçüktabak, S. J. Kim, Y. Wen, K. Lynch, J. L. Pons, Human-machine-human interaction in motor control and rehabilitation: a review, *Journal of NeuroEngineering and Rehabilitation* **18**, 183 (2021).
17. E. L. Waters, R. J. Mendonca, P. Z. Cacchione, M. J. Johnson, *2024 10th IEEE RAS/EMBS International Conference for Biomedical Robotics and Biomechatronics (BioRob)* (IEEE, 2024), pp. 1498–1503.
18. G. Ganesh, *et al.*, Two is better than one: Physical interactions improve motor performance in humans, *Scientific Reports* (2014).
19. A. Takagi, G. Ganesh, T. Yoshioka, M. Kawato, E. Burdet, Physically interacting individuals estimate the partner's goal to enhance their movements, *Nature Human Behaviour* **1** (2017).

20. N. Beckers, E. H. F. van Asseldonk, H. van der Kooij, Haptic human–human interaction does not improve individual visuomotor adaptation, *Scientific Reports* **10**, 19902 (2020).
21. A. Takagi, F. Usai, G. Ganesh, V. Sanguineti, E. Burdet, Haptic communication between humans is tuned by the hard or soft mechanics of interaction, *PLoS Computational Biology* **14**, 1 (2018).
22. E. J. Avila Mireles, J. Zenzeri, V. Squeri, P. Morasso, D. De Santis, Skill learning and skill transfer mediated by cooperative haptic interaction, *IEEE Transactions on Neural Systems and Rehabilitation Engineering* **25**, 832 (2017).
23. S. Kager, *et al.*, The effect of skill level matching in dyadic interaction on learning of a tracing task, *IEEE International Conference on Rehabilitation Robotics* **2019-June**, 824 (2019).
24. S. J. Kim, *et al.*, A framework for dyadic physical interaction studies during ankle motor tasks, *IEEE Robotics and Automation Letters* **6**, 6876 (2021).
25. S. J. Kim, *et al.*, Effect of dyadic haptic collaboration on ankle motor learning and task performance, *IEEE Transactions on Neural Systems and Rehabilitation Engineering* **31**, 416 (2023).
26. M. R. Short, *et al.*, Haptic human-human interaction during an ankle tracking task: Effects of virtual connection stiffness, *IEEE Transactions on Neural Systems and Rehabilitation Engineering* **31**, 3864 (2023).
27. M. R. Short, *et al.*, Effects of uni- and bidirectional interaction during dyadic ankle and wrist tracking, *IEEE Transactions on Neural Systems and Rehabilitation Engineering* (2025).

28. E. B. Küçüktabak, *et al.*, 2023 *International Conference on Rehabilitation Robotics (ICORR)* (2023), pp. 1–6.
29. L. Vianello, *et al.*, 2024 *IEEE International Conference on Robotics and Automation (ICRA)* (IEEE, 2024), pp. 4521–4527.
30. M. H. Koh, *et al.*, Exploiting telerobotics for sensorimotor rehabilitation: a locomotor embodiment, *Journal of NeuroEngineering and Rehabilitation* **18**, 1 (2021).
31. G. A. BORG, Psychophysical bases of perceived exertion, *Medicine & Science in Sports & Exercise* **14** (1982).
32. E. McAuley, T. Duncan, V. V. Tammen, Psychometric properties of the intrinsic motivation inventory in a competitive sport setting: A confirmatory factor analysis, *Research quarterly for exercise and sport* **60**, 48 (1989).
33. T. M. Sukal, J. P. Dewald, M. D. Ellis, 2005 *IEEE Engineering in Medicine and Biology 27th Annual Conference* (IEEE, 2006), pp. 5032–5035.
34. H. Tanaka, K. D. Monahan, D. R. Seals, Age-predicted maximal heart rate revisited, *Journal of the american college of cardiology* **37**, 153 (2001).
35. G. Chen, C. Patten, D. H. Kothari, F. E. Zajac, Gait differences between individuals with post-stroke hemiparesis and non-disabled controls at matched speeds, *Gait & posture* **22**, 51 (2005).
36. D. C. Kerrigan, E. P. Frates, S. Rogan, P. O. Riley, Spastic paretic stiff-legged gait: Biomechanics of the unaffected limb: 1, *American journal of physical medicine & rehabilitation* **78**, 354 (1999).

37. H. Souissi, R. Zory, J. Bredin, N. Roche, P. Gerus, Co-contraction around the knee and the ankle joints during post-stroke gait, *European journal of physical and rehabilitation medicine* **54** (2018).
38. H. Lim, B. Cleland, S. Madhavan, Functional connectivity of proximal and distal lower limb muscles and impact on gait variability in stroke, *Gait & posture* **99**, 20 (2023).
39. M. M. Ouellette, *et al.*, High-intensity resistance training improves muscle strength, self-reported function, and disability in long-term stroke survivors, *Stroke* **35**, 1404 (2004).
40. H. Hsiao, B. A. Knarr, J. S. Higginson, S. A. Binder-Macleod, Mechanisms to increase propulsive force for individuals poststroke, *Journal of neuroengineering and rehabilitation* **12**, 1 (2015).
41. L. Amato, *et al.*, Unidirectional human-robot-human physical interaction for gait training, *arXiv preprint arXiv:2409.11510* (2024).
42. K. L. Poggensee, S. H. Collins, How adaptation, training, and customization contribute to benefits from exoskeleton assistance, *Science Robotics* **6**, eabf1078 (2021).
43. J. Fong, *et al.*, CANopen Robot Controller (CORC): An open software stack for human robot interaction development, *The International Symposium on Wearable Robotics (WeRob2020)* **2020** (2020).
44. Y. Li, Q. Wei, W. Gou, C. He, Effects of mirror therapy on walking ability, balance and lower limb motor recovery after stroke: a systematic review and meta-analysis of randomized controlled trials, *Clinical rehabilitation* **32**, 1007 (2018).
45. E. B. Küçüktabak, *et al.*, Haptic transparency and interaction force control for a lower limb exoskeleton, *IEEE Transactions on Robotics* **40**, 1842 (2024).

46. E. Tarihci Cakmak, A. Yaliman, G. Torna, E. I. Sen, The effectiveness of bodyweight-supported treadmill training in stroke patients: randomized controlled trial, *Neurological Sciences* **45**, 3277 (2024).

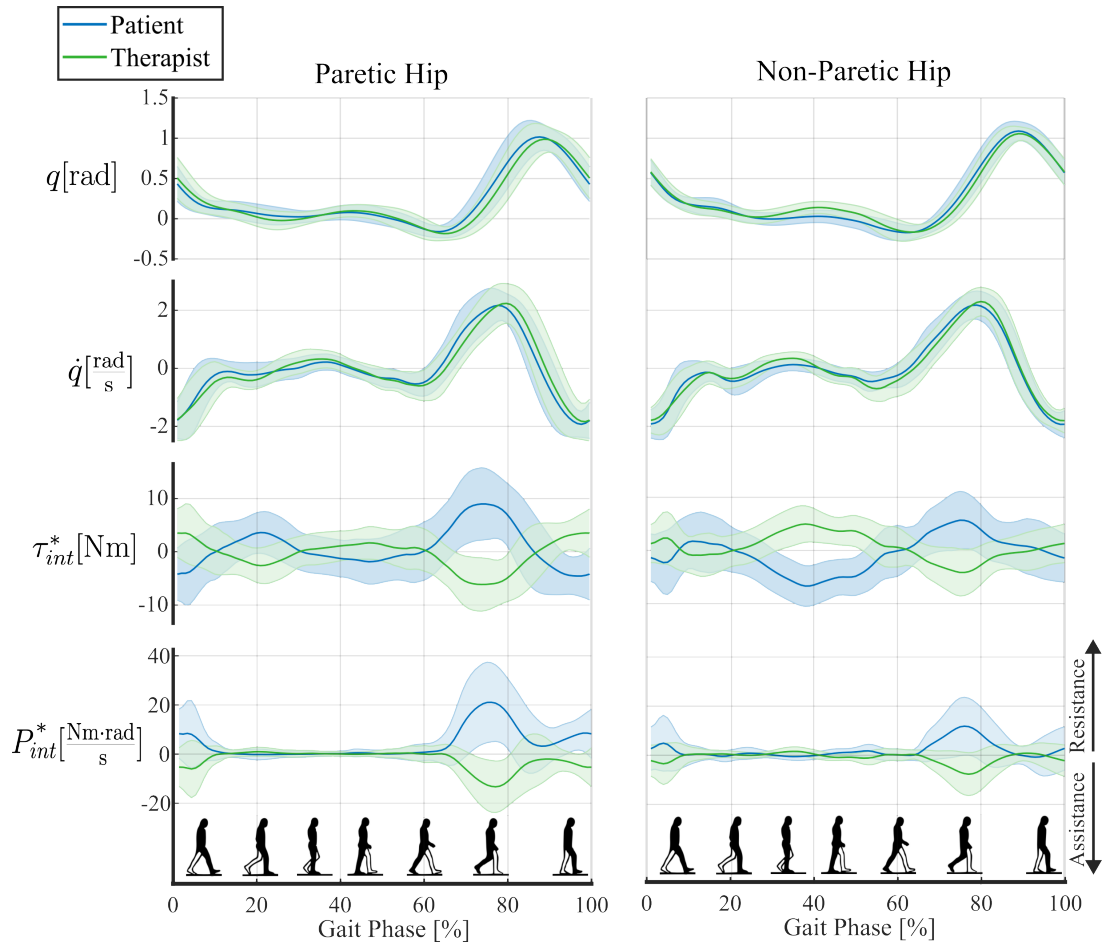
Supplementary Materials

Patient	Training Block 1 (10 mins)		Training Block 2 (10 mins)		Training Block 3 (10 mins)	
	K_p [$\frac{\text{Nm}}{\text{rad}}$]	K_t [$\frac{\text{Nm}}{\text{rad}}$]	K_p [$\frac{\text{Nm}}{\text{rad}}$]	K_t [$\frac{\text{Nm}}{\text{rad}}$]	K_p [$\frac{\text{Nm}}{\text{rad}}$]	K_t [$\frac{\text{Nm}}{\text{rad}}$]
U1	49	49	49	49	49	49
U2	49	49	49	49	-	-
U3	49	49	58	49	58	49
U4	64	64	49	49	49	49
U5	49	49	49	49	49	36
U6	49	49	49	25	49	25
U7	60	60	60	60	60	60
U8	60	60	60	45	60	30

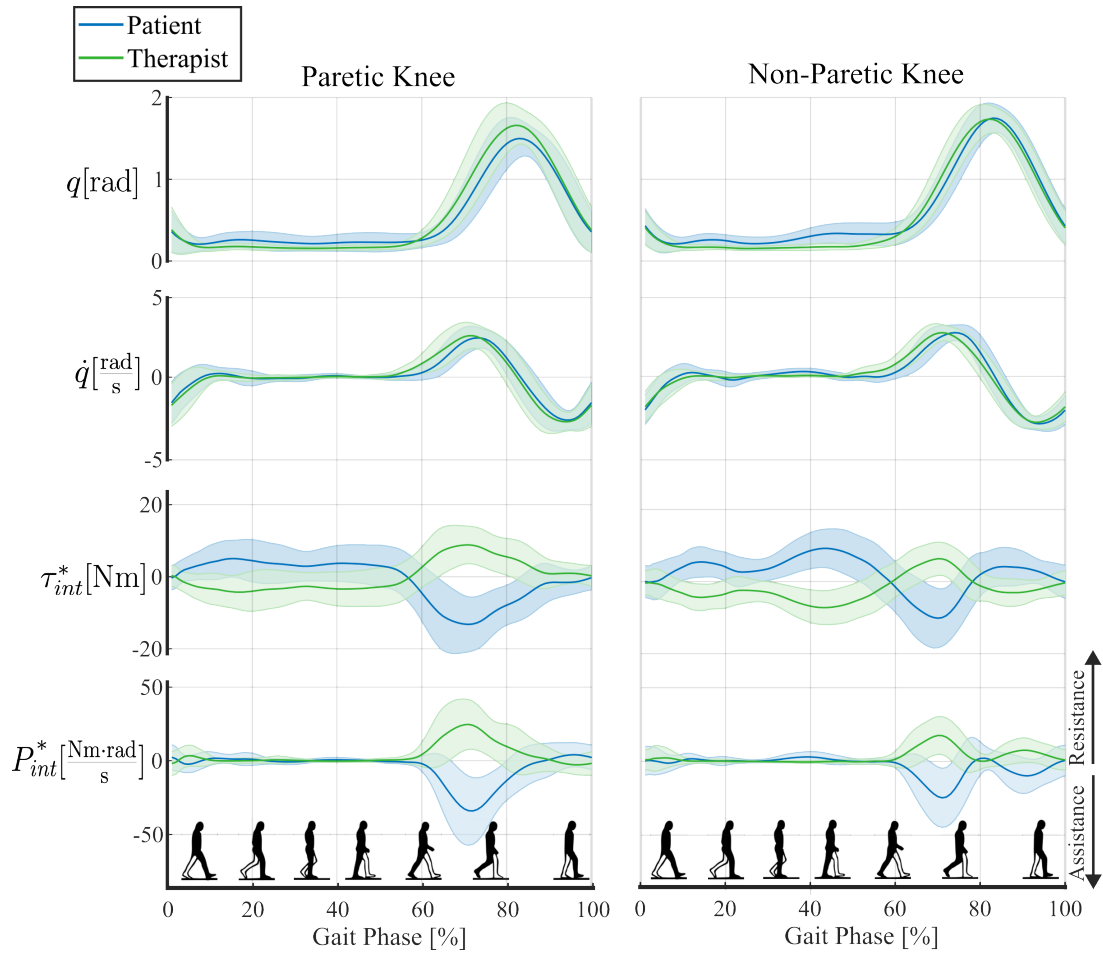
Supplementary Table 1: Stiffness combinations across training blocks for each patient. The therapist dictated stiffness changes by requesting more or less feedback from the patient—adjusting K_t accordingly—and by modulating haptic feedback transmitted to the patient through changes in K_p . Patient U2 performed only two of the three blocks due to a technical issue with the robotic system.

0.1 Dataset description

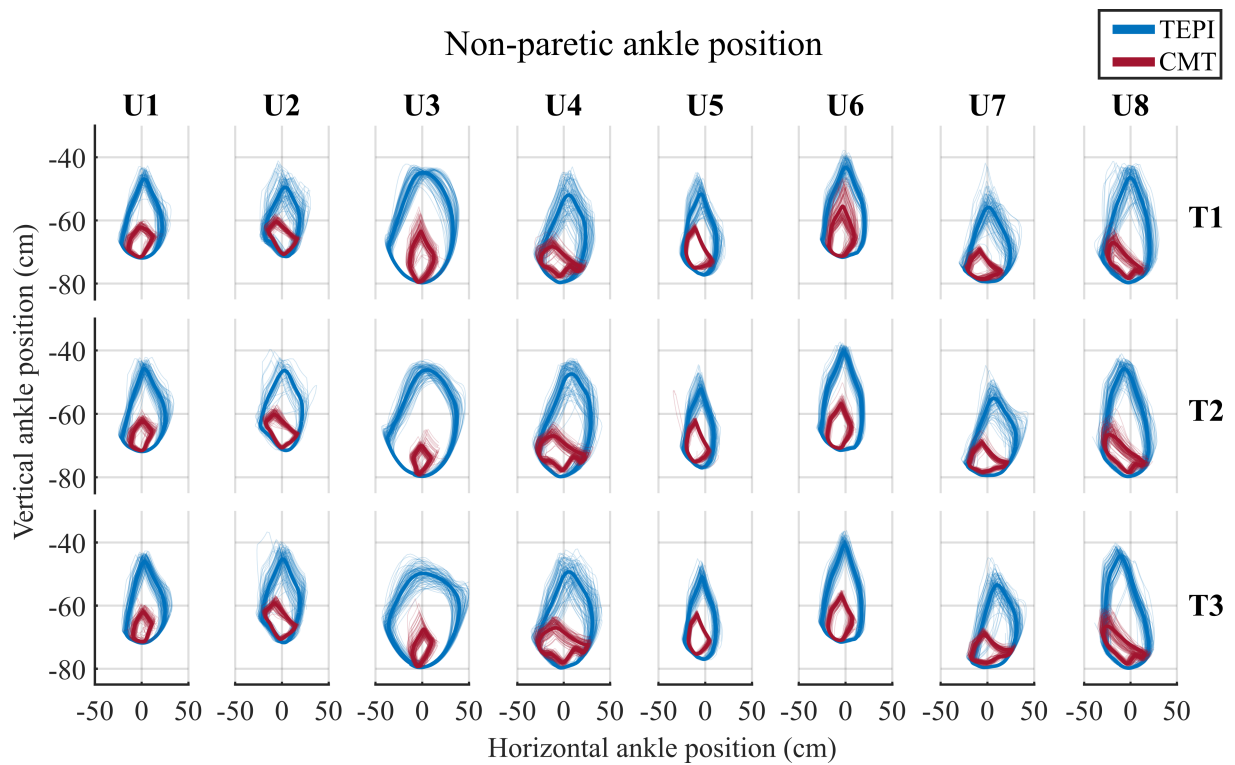
The associated dataset is available as supplemental material and can be accessed through the provided link (Dataset). Included with the dataset are sample MATLAB scripts and a README.md file to guide readers on how to use the data (GitHub of the available code).



Supplementary Figure 1: Kinematic and dynamic motion of the hip joints (paretic and non-paretic) for all dyadic interaction, grouped. From top to bottom, the plots show: joint position, joint velocity, rendered interaction torque, and interaction power. Patient data are shown in blue, while therapist data are shown in green. The left column displays measurements for the paretic hip, and the right column for the non-paretic hip.



Supplementary Figure 2: Kinematic and dynamic motion of the knee joints (paretic and non-paretic) for all dyadic interaction, grouped. From top to bottom, the plots show: joint position, joint velocity, rendered interaction torque, and interaction power. Patient data are shown in blue, while therapist data are shown in green. The left column displays measurements for the paretic knee, and the right column for the non-paretic knee.



Supplementary Figure 3: Non-paretic limb ankle trajectories for each patient (U1-U8) across training blocks (T1-T3), compared between the two training types: exoskeleton (dyad) and conventional (conv).